IFSCC 2025 full paper (IFSCC2025-1361)

"Optimizing Active Ingredient Delivery in Personalized Cosmetics by Modulating Flexibility through Liposome Structural Modifications"

Minjoo Noh[1†], Quynh Nguyenb[2†], Minji Song[2], Jihyun Lee[1], Seoyoon Lee[1], Heemuk Oh[1], Sung Yun Hong[1], Jihui Jang[1], Chun Ho Park[1], Young-bok Lee[2*], Jun Bae Lee[1*]

[1]R&I Center, COSMAX, Seongnam-si, Republic of Korea; [2]Department of Applied Chemistry, Hanyang University, Ansan-si, Republic of Korea

1. Introduction

Liposomes are advanced delivery systems capable of simultaneously encapsulating both hydrophobic and hydrophilic active agents, and have been extensively developed for cosmetic applications. To meet specific functional needs, it is equally important to modulate the transdermal delivery of these active ingredients. One promising strategy involves modifying the liposomal membrane by incorporating fatty alcohols, whose effectiveness is closely related to the length of their alkyl chains **[1-3]**. While most of previous studies have investigated the incorporation of fatty alcohols into various lipid-based vesicular systems, they have primarily focused on the interaction between fatty alcohols and the skin **[1,3-6].** In contrast, their impact on the structure, flexibility, and dynamic behavior of liposomes remains underexplored. In this study, we examine how fatty alcohols with varying alkyl chain lengths influence liposomal structure—particularly membrane flexibility, which is strongly associated with transdermal delivery performance.

For this purpose, the two liposomes were prepared with the inclusion of two commonly used fatty alcohols in the cosmetic field—cetyl alcohol and behenyl alcohol. These alcohols differ in their carbon chain lengths, which is expected to significantly affect their physicochemical characteristics and, consequently, modulate the structural integrity and flexibility of liposomal membranes. Here, these liposome samples will be used to co-deliver ceramide and niacinamide, two widely used active agents in cosmetic formulations known for their well-documented skin benefits. Ceramide plays a vital role in maintaining skin barrier integrity and hydration **[7-9]**, while niacinamide—a biologically active form of vitamin B3—offers broad dermatological benefits, including anti-inflammatory, antioxidant activities **[10,11]**. It is also recognized as an effective skin-brightening agent, capable of reducing hyperpigmentation **[12,13]**. The selection of ceramide and niacinamide as active agents in this study is based on their well-established therapeutic potential, coupled with the significant challenges associated with their transdermal delivery due to intrinsic physicochemical properties. Ceramide is hydrophobic substance which

is unstable, and prone to crystallization, **[13]** while niacinamide is highly hydrophilic that exhibits poor skin penetration **[14-16]**. Liposomes present a promising strategy to address these limitations by improving the stability and delivery efficiency of both compounds. However, the potential of fatty alcohol-modified liposomes for the co-delivery of ceramide and niacinamide—particularly within cosmetic applications—remains insufficiently explored.

Here, beyond examining the effects of fatty alcohols on liposome structure and the delivery efficiency of ceramide and niacinamide, we also evaluated the application potential of the resulting liposomal formulations for skin barrier reinforcement and brightening, using artificial skin models and advanced analytical techniques. The skin barrier-enhancing effects of the formulations were evaluated using small-angle X-ray scattering (SAXS) and high-resolution magic angle spinning nuclear magnetic resonance (HR-MAS NMR), while their brightening efficacy was assessed through in vitro studies with a 3D-reconstructed pigmented epidermis model and Fontana–Masson staining. This comprehensive study—from structural characterization to functional evaluation—provides valuable insights into how long-chain fatty alcohols influence liposome structure, permeability, and performance, offering a solid foundation for designing advanced liposomal formulations to improve skin health and address diverse skincare needs..

2. Materials and Methods

2.1. Materials

Ceramide-NP (Doosan, Korea), hydrogenated lecithin (Lipoid Kosmetik, Germany), glycerin (Edenor Oleochemicals, Malaysia), cholesterol (Active Concepts, USA), niacinamide (Shandong Kunda Biotechnology, China), C12-20 alkyl glucoside (Montanov L) (Seppic S.A., France), cetyl alcohol (BASF, Germany), behenyl alcohol (BASF, Germany), stearic acid (Sigma-Aldrich, Germany), fluorescein-5-isothiocyanate (FITC) (Sigma-Aldrich, Germany), 4′,6-diamidino-2-phenylindole dihydrochloride (DAPI) (Sigma-Aldrich, Germany), and α-melanocyte-stimulating hormone (α-MSH) (Sigma-Aldrich, Germany) were purchased from Sigma-Aldrich. EpiDerm EPI-200 was purchased from MatTek Corporation. RHPE (Reconstructed Human Pigmented Epidermis) Brown (Phototype VI) (SkinEthic) was procured from Episkin Laboratories (France). O.C.T. compound was obtained from Sakura Finetek. All materials were of analytical grade, and deionized, double-distilled water was used for all experiments**.**

2.2. Preparation of liposome formulation without fatty alcohol (C0), with Cetyl Alcohol incorporation (C16) and Behenyl Alcohol incorporation (C22)

For the preparation of lipid particle formulations, predetermined amounts of ceramide, cholesterol, stearic acid, cetyl alcohol (for C16) and behenyl alcohol (for C22), C12-20 alkyl glucoside, and lecithin were melted at 80°C. Then, the molten phase was injected into the aqueous solution, and the mixture was stirred using a mixer (Agi-mixer, HY-002, Hansung ENG, Korea) for 20 min. The formulation was subsequently subjected to sonication with a probe-type sonicator (Q700, QSonica LLC., Newton, CT, USA). Sonication was performed for a total of 15 min, consisting of three cycles of 5 min each with intervals of 10 s ‘on’ and 5 s ‘off’. The final formulation was completed by filtration through a 0.45 μm filter (Minisart CA 26 mm).

2.3. Lipsome structural characterization

The structural analysis of the liposome interface was performed using wide-angle X-ray scattering (WAXS). WAXS measurements were conducted at the 4C beamline of a third-generation radiation accelerator, utilizing a 3 GeV beam from the Pohang Light Source II (PLS II) at Pohang Accelerator Laboratory (Korea). The experiments were performed at room temperature using an FP50-HL refrigerated simulator (JULABO), with each sample measured for 10 s and averaged over six replicates. Data were averaged over half-circle echoes and normalized for transmitted light intensity.

Solution-state ^{1}H NMR spectra were recorded at 25°C using a Bruker 400 MHz NMR spectrometer. To further investigate the structural flexibility of the liposome samples, T_2 relaxation times were measured at 25°C. A single pulse sequence with solvent pre-saturation at 4.7 ppm (to suppress the water signal) and a Carr-Purcell-Meiboom-Gill (CPMG) sequence were employed to mitigate the effects of water. Data were processed with a line broadening of 0.3 Hz. The ^{1}H-NMR spectra were processed using Topspin 3.6 software, with chemical shifts referenced to the TMSP-d_4 signal at 0 ppm.

2.4. In vitro skin permeation study

The permeation efficiency of niacinamide and ceramides was studied using Franz diffusion cell and Strat-M membrane (Transdermal diffusion test model, 25 mm, Merck). The receptor compartment was filled with PBS:ethanol (1:1, v/v), maintained at 32 ± 0.5 °C, and stirred at 350 rpm. A 200 µL aliquot of each sample was applied to the donor compartment. After 2, 4, 8, and 24 h, 1 mL of receptor fluid was collected and replaced with fresh medium. Permeated niacinamide was quantified by high-performance liquid chromatography (HPLC, Ultimate 3000, Dionex) using a C18 column (Jupiter, 5 µm, 250 × 4.6 mm) with a mobile phase of 10 mM KH2PO4/acetonitrile (93:7), flow rate 1 mL/min, and detection at 263 nm. Ceramide was analyzed via LC-MS/MS using a ZORBAX Eclipse C18 column (3.5 µm, 2.1 × 100 mm) and a mobile phase of 10 mM ammonium acetate:ACN:IPA (20:35:45), flow rate 0.3 mL/min, injection volume 5 µL, and ESI-positive mode (m/z 582.6 → 564.7, 300.4, 282.4). All data were averaged from three replicates.

The skin penetration of liposome formulations were observed via confocal laser scanning microscopy. Prior applied onto 3D skin tissue (EpiDerm EPI-200, MatTek Corporation), the formulations was incorporated with fluorescence dye (FITC, green) at concentration of 0.003 wt%. A 30 µL aliquot of each FITC-containing liposome formulation was gently applied to the surface of 8 mm diameter 3D skin tissue. After 4h, the samples were fixed in formalin and stained with DAPI before frozen. The nuclei of the stained 3D skin samples were visualized using confocal laser scanning microscopy (CLSM) at Kangwon National University. Excitation of FITC and DAPI was performed at 488 and 408 nm, respectively.

4.6. In vitro skin barrier enhancement efficacy study

The Epiderm EPI-200 3D skin model (MatTek) with diameter of 8 mm were incubated for 1h before treated with 30 µL of liposome formulations and kept in formalin solution after 24h. The skin barrier assessment was carried out using Small-Angle X-ray Scattering (SAXS) with a sample-to-detector distance of 2 m and a scattering vector range of 0.015 $Å^{-1}$ <q<0.25 $Å^{-1}$. The samples were measured as thin films attached to a multi-sample stage.

High-resolution magic angle spinning (HR-MAS) NMR experiments were conducted on a Bruker NMR spectrometer operating at 400 MHz for ^{1}H with a HR-MAS probe and spinning

rate of 7 kHz. For sample preparation, 60 µL of each formulation was applied to artificial skin that was purchased from MatTek Corporation and were left to set for 24 h. A single pulse sequence with solvent pre-saturation at 4.7 ppm (to suppress the water signal) and a CPMG sequence was used for data collection. All the data were processed with a line broadening of 0.3 Hz. The HR-MAS NMR spectra were analyzed using Topspin 3.6 software, with chemical shifts referenced to the TMSP-d4 signal at 0 ppm.

4.5. In vitro skin lightening study

A 40 µL of liposome formulations were applied in different, reconstructed human pigmented epidermis (RHPE; SkinEthic-Brown, Phototype VI, EPISKIN, France) and incubate for 24 h. Then, melanin distribution in the tissue cross-sections was visualized using Fontana–Masson stain and optical microscopy. Alongside, the long-term experiment were conducted with the daily application of formulations during one week, the untreated and treated samples were then evaluated via microscopic images.

3. Results

3.1. Characterization of Liposome Samples

In this study, liposomal formulations were prepared without fatty alcohols (C0) and with the incorporation of cetyl alcohol (C16) or behenyl alcohol (C22) to investigate the impact of fatty alcohol chain length on liposome structure and flexibility. Structural characterization was conducted using wide-angle X-ray scattering (WAXS).

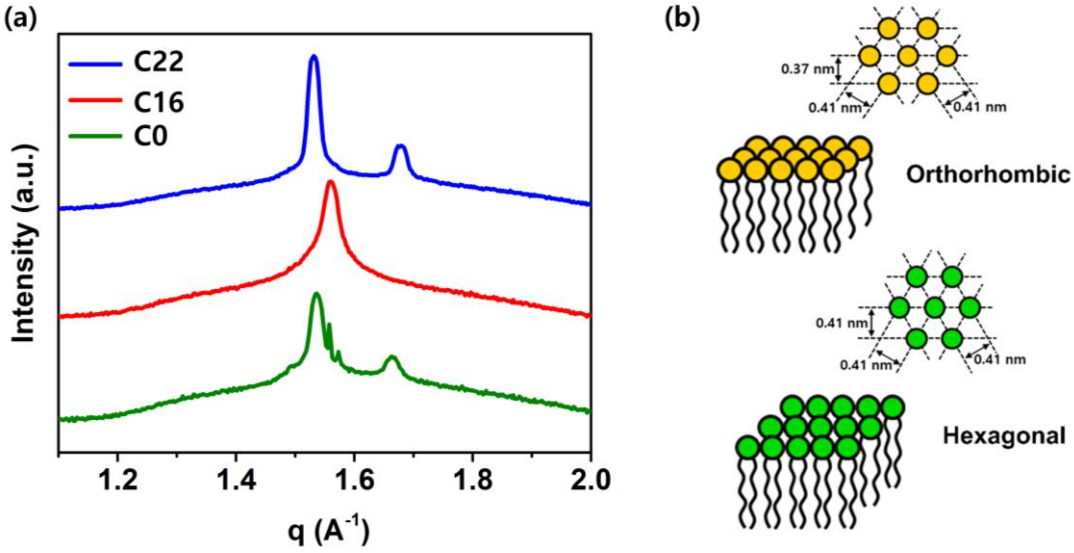

Figure 1. (a) Wide-angle X-ray scattering (WAXS) patterns of C0, C16, and C22 liposomes; (b) Interfacial structural arrangements of the phospholipid bilayer: orthorhombic and hexagonal.

As shown in Figure 1, the WAXS spectra of the C22 formulation exhibited two distinct Bragg peaks at approximately 1.53 $Å^{-1}$ and 1.68 $Å^{-1}$, corresponding to d-spacing values of 0.41 nm and 0.37 nm, respectively. In contrast, the C16 formulation displayed a single peak at ~1.55 $Å^{-1}$, corresponding to a d-spacing of 0.41 nm. These reults indicated that C16 and C22 possess the two different membrane structure, where C16 has hexagonal packing while C22 exhibits orthorhombic arrangement, according to Bragg's Law. Notably, additional minor peaks were observed in the spectrum of the C0 formulation, suggesting the presence of crystallized

or precipitated components. This contrasts with the spectra of C16 and C22, which showed no evidence of active ingredient precipitation. These findings indicate that the incorporation of fatty alcohols, particularly C16 and C22, enhances the stability of the formulation, enabling the successful encapsulation of a relatively high concentration (0.1 wt%) of ceramide—a compound typically challenging to stabilize in liquid systems.

In addition to WAXS, the structure flexibility of liposomes was also study by ^{1}H NMR with a focusing on spin–spin relaxation times (T_2) to assess the dynamic behavior associated with membrane packing density. To enable accurate interpretation of the T_2 relaxation data, the 1D ^{1}H-NMR spectra were first recorded for the assignment of proton peaks belong to nanoliposome structure. To support the assignments, the ^{1}H NMR for primary ingredients used for liposome preparation, including Montanov-L surfactant and fatty alcohols, were also collected (Figure 2). The spectra of cetyl alcohol and behenyl alcohol displayed characteristic peaks in two distinct regions: a signal near 3.6 ppm corresponding to the methylene protons adjacent to the hydroxyl group (–CH_2OH), and broader peaks in the 0.8–1.7 ppm range attributed to the protons along the long alkyl chains. For Montanov-L spectrum, peaks within 3.35–4.00 ppm were assigned to protons of the glucose rings, the peak at 3.24 ppm to the methylene group adjacent to the glycosidic linkage (–CH_2O–), and peaks between 1.2–1.7 ppm and at 0.9 ppm to methylene and terminal methyl protons of the alkyl chains, respectively **[17,18]**. By comparison the spectra of raw materials with those of nanoliposome, the liposomal ^{1}H NMR signals were divided to three main region: hydrophilic head (3.35–4.00 ppm), bridge (3.24 ppm) and hydrophobic tail (0.8–1.7 ppm) for further analyis.

Following the assignment, the T_2 relaxation time of fatty alcohol-incorporated nanoliposome samples were studied across the three regions to evaluate the change in structural flexibility (Table 1). Overall, the T_2 values obtained for three main region of liposomes are greater for C16 sample, indicating the higher mobility and flexibility of this sample compared to C22.

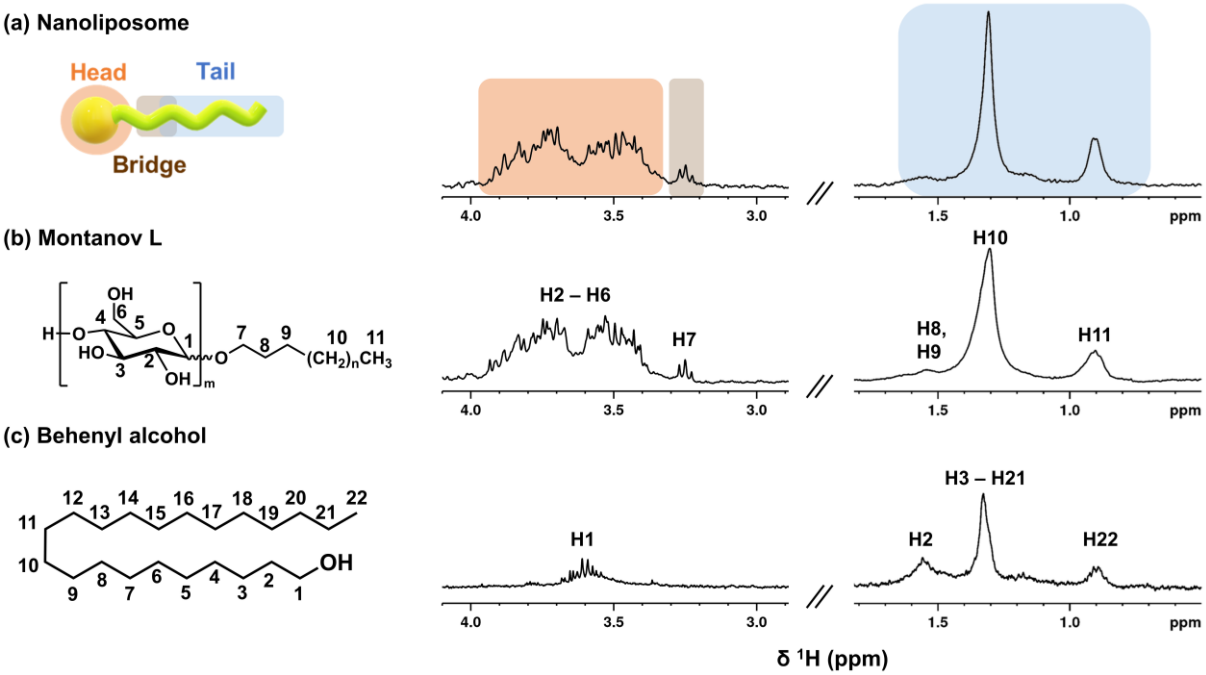

Figure 2. ^{1}H-NMR spectra of nanoliposomes and their raw materials.

Table 1. T_2 values for C16 and C22 liposomes at room temperature. (Unit: ms)

Sample	Head	Bridge	Tail
C16	367.5 ± 9.40	485.4 ± 26.8	117.9 ± 1.8

C22	309.3 ± 23.4	436.6 ± 23.1	111.0 ± 2.5

3.2. In vitro Skin Permeation

Following the structural and flexibility characterization of the liposome samples, their skin permeation performance was evaluated. First, an *in vitro* study using Franz diffusion cells was conducted with artificial synthetic membrane and the analysis was performed with HPLC and LC/MSMS system for niacinamide and ceramide, respectively. As can be seen from Figure 3a, the analysed results showed that both C16 and C22 formulation exhibits better skin permeation of ceramide and niacinamide at all the time point (after 2, 4, 8 and 24 h application) in comparison with formulation of liposome without fatty-alcohol modification. In addition, the skin penetration test of the investigated formulation (C16 and C22) was also conducted with confocal laser scanning microscopy (CLSM) (Figure 3b). The results revealed that the C16 formulation achieved a greater penetration depth, with a 1.6-fold increase in the penetration area compared to the C22 formulation.

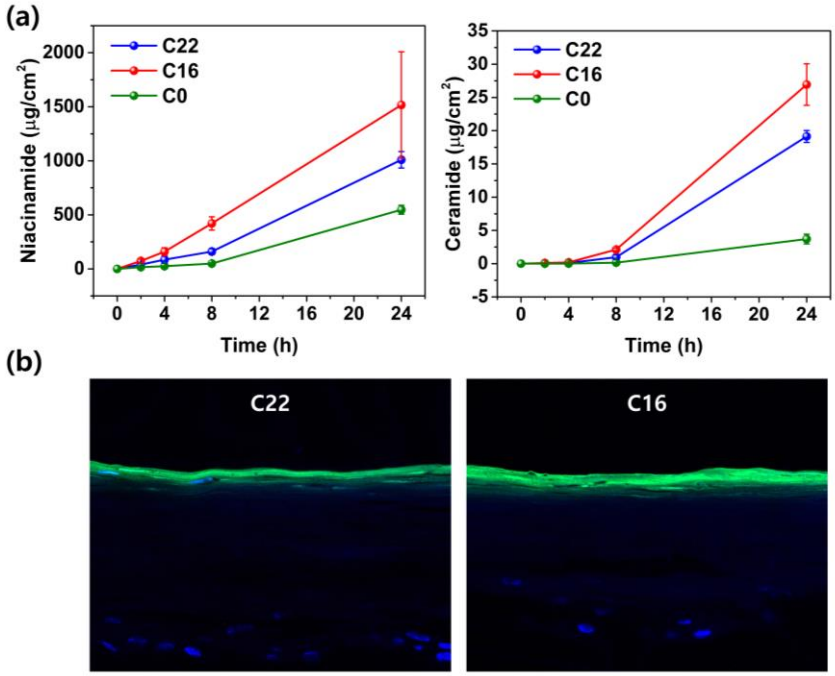

Figure 3. (a) *In vitro* diffusion profiles of niacinamide (left) and ceramide (right) through an artificial synthetic membrane (Strat-M); (b) Cross-sectional confocal laser scanning micrographs (CLSM) for C22 formulation- and C16 formulation-treated 3D skin tissues.

3.2. Evaluate Skin Barrier Function Enhancement

After extensively study about the structure and skin permeability of C16 and C22 liposomes, their performance efficiency in enhancing skin barrier was evaluated in which small-angle X-ray scaterring measurements were conducted. The obtained spectra, as shown in Figure 4a, revealed a more pronounced lamellar structure in the artificial skin samples treated with C16 and C22 formulations compared to the untreated sample (control), with the most prominent in the C16-treated skin.

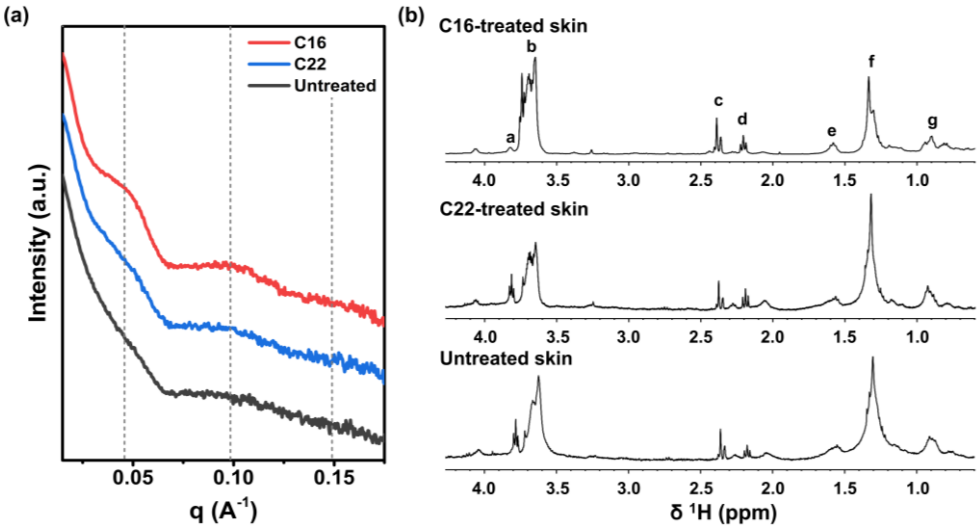

Figure 4. (a) SAXS patterns (Kratky plot) of stratum corneum sheets from an untreated EpiDerm artificial skin and skin treated with C16 and C22. (b) HR-MAS ^{1}H NMR spectra of untreated (control) artificial skin and skin treated with C16 and C22.

Along with SAXS, HR-MAS NMR technique was also utilized for additional insights about the changes in skin properties upon treatment with C16 and C22 compared to untreated skin, with a particular focus on T_2 relaxation measurements. Prior the T_2 relaxation time analysis, the ^{1}H HR-MAS NMR spectra of skin samples were recored for the peak assignment, based on previous studies **[19-24],** the assignment with peak mark a-g were shown in Figure 5. Since signal b in Figure 4b of treated samples is presumed to overlap with residue Montanov L surfactant, subsequent analysis of T_2 relaxation time of NMR signals focused on signal a and c-g. The results revealed that most signals in the C16- and C22-treated samples exhibited shorter T_2 values compared to the untreated control, indicating enhanced skin structural integrity (Figure 5). In addition, a comparison between the values between C16-treated skin and C22-treated sample, it is clear that most of the signals possess the shorter T_2 in C16-treated case. This result implies the more pronounced effect of C16 on the skin structure, potentially contributing to improved epidermal defense system against environmental stress.

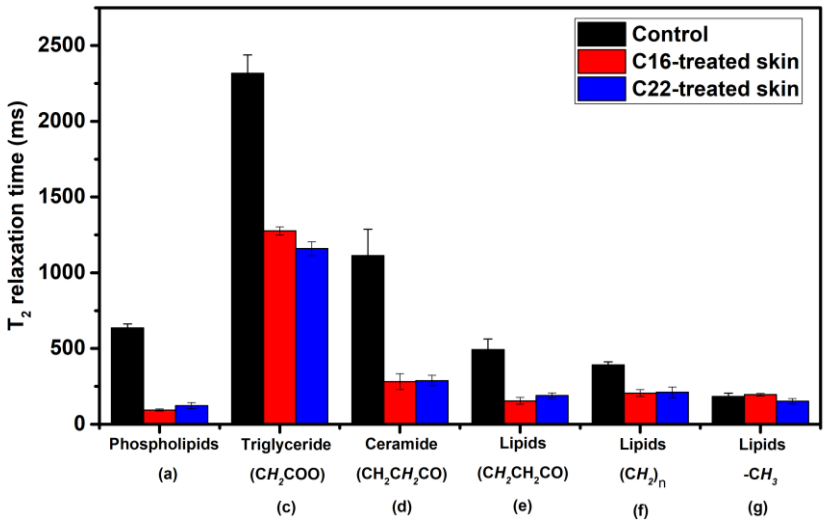

Figure 5. Comparative analysis of T_2 values for key skin components in untreated skin (control), C16-treated, and C22-treated samples.

3.4. In vitro Skin Lightening

In order to assess the skin whitening effect of the liposome formulation, we conducted the experiment using reconstructed human pigmented epidermis (RHPE) which appears pigmented due to the presence of melanocytes. For the clear comparison, besides C16 and C22 formulations, the niacinamide solution with 2% of niacinamide was also used and untreated skin was used as control sample. After short-term application, the analysis of Fontana–Masson-stained histological sections of 3D skin tissues demonstrated the superior melanin migration suppression of C16 and C22, especially C16-treated sample (Figure 6a). After one week of treatment, the sample treated with the niacinamide solution and the nanoliposome formulations showed an increase in the skin lightness, while a decrease was observed for the untreated sample. Specifically, C16 appeared brightest under the microscope (Figure 6b), making it the most effective formulation for skin lightening.

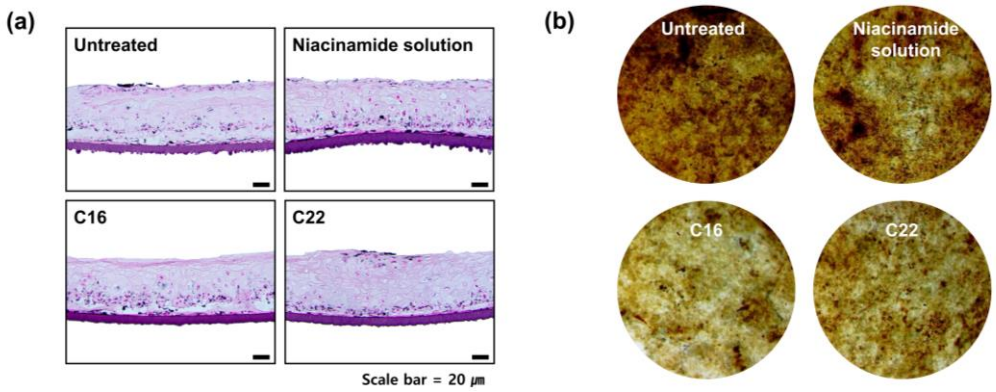

Figure 6. (a) Cross-sectional images showing pigmentation observed through Fontana–Masson (FM) staining of untreated and treated RHPE samples. (b) Microscopic images of untreated and treated RHPE samples.

4. Discussion

From WAXS measurements (Figure 1), it is evidenced that the C22 formulation adopts an orthorhombic arrangement, characterized by a more tightly packed structure, whereas the C16 formulation exhibits a hexagonal arrangement, which is inherently more loosely packed and thus allows for greater interfacial flexibility **[25]**. This structural distinction is in good agreement with ^{1}H NMR characterization data (Table 1), where the C16 formulation showed longer T_2 relaxation times, indicative of higher molecular mobility and membrane flexibility. The more rigid structure of C22 can be attributed to the stronger van der Waals interaction arising from its longer alkyl chains **[26-28]**. Noticably, the incorporation of fatty alcohols was also found to play a critical role in stabilizing ceramide within the liposomal membrane. This stabilization is likely due to enhanced hydrophobic interactions facilitated by the fatty alcohols, which help prevent ceramide crystallization.

With the ability to suppress the crystallization of ceramide and adjust skin flexibility based on the use of fatty alcohol with different chain length, the permeability of active agents is expected to be influenced. Indeed, the LC analysis has shown that with fatty alcohol inclusion in liposome structure, the skin permeation of niacinamide and ceramide are significantly improved (Figure 3a). These results can be attributed to the ceramide stabilization and ability to disrupt the tightly packed lipids occupy space in stratum corneum. Additionally, over time, the C16 formulation consistently exhibited the highest permeation rate through the artificial membrane among the

three tested samples. Besides, the penetration examination with CLSM measurement, as shown in Figure 3b, also confirmed the greater penetration area of C16 compared to C22. This enhanced performance is likely due to the greater structural flexibility of the C16 formulation, which facilitates deeper and faster penetration into the skin layers.

Owings to the improved skin permeability, the skin application of the C16 and C22 formulation provide the significant change in skin structure. The more pronounced lamellar structure observed in SAXS implies that the formulation can strengthen the skin barrier **[13]**, with C16 demonstrating the most significant effect (Figure 4a). The results here is highly consistent with the data obtained in HR-MAS measurement (Figure 5), where the decrease in T_2 values of skin signals indicates the reinforcement of a well-constructed skin barrier. This observation is due to the supplement of ceramide, which plays important role in maintaining skin lipid barrier **[7-9]**, via C22 and C16 liposome formulations. Besides, compared to C22, the C16 showed superior skin strengthening performance. This is attributed to the enhanced skin permeability of the C16 formulation, driven by its higher liposome fluidity and its ability to facilitate deeper penetration into the skin layers, as confirmed by the skin permeation study in the previous section, where the C16 demonstrated superior penetration compared to the C22 formulation.

Along with ceramide, the niacinamide as the other active agent was also deliveried into skin more effectively. This could be seen from the comparison of sample treated with C16 and C22 liposome formulations with solution of 2% niacinamide. Being accommodated in the liposome hydrophilic core, niacinamide can be penetrated deeper into skin layer to delivery its bioefficacy. Additionally, the more flexible liposome formulation (C16) also show here the better effect in skin whitening owings to the enhanced skin penetration.

5. Conclusion

This study highlights how modulating liposome membrane flexibility through fatty alcohol incorporation can optimize active ingredient delivery in personalized cosmetics. Both C22 (behenyl alcohol) and C16 (cetyl alcohol) significantly stabilize ceramide within the liposome structure, preventing crystallization and ensuring formulation integrity. Specifically, C16, with its more flexible hexagonal packing, also enhanced skin penetration and interaction, improving the delivery of both ceramide and niacinamide. On the other hand, behenyl alcohol (C22), with longer chain length, induces a more rigid membrane structure due to stronger van der Waals interactions between its extended hydrophobic chains, which enhances the stability of the liposome bilayer and reduces permeability in comparison to C16. Overall, This study underscores the importance of chain length variations in liposome properties, enabling precise adjustments to membrane characteristics for optimizing formulations in targeted delivery, enhanced skin permeability, and controlled release of active agents.

References

1. N. Kanikkannan, M. Singh, Int. J. Pharm. 2002, 248, 219;
2. R. J. Babu, L. Chen, N. Kanikkannan, in (Eds: N. Dragicevic, H. I. Maibach), Springer, Berlin Heidelberg, Berlin, Heidelberg 2015.
3. V. Sanna, G. Caria, A. Mariani, Powder Technol. 2010, 201 (1), 32.
4. S. Andega, N. Kanikkannan, M. Singh, J. Control. Release. 2001, 77, 17.
5. A. Kováčik, M. Kopečná, I. Hrdinová, L. Opálka, M. Boncheva Bettex, K. Vávrová, Mol. Pharm. 2023, 20, 6237.
6. J. Klimentová, P. Kosák, K. Vávrová, T. Holas, A. Hrabálek, Bioorg. Med. Chem. 2006, 14, 7681.

7. D. Gan; Q. Wang, X. Zhang, X. Qu, H. Sun, Y. Cui, W. Wang, L. Qu, X. Dong, Adv. Funct. Mater. 2024, 2411588.
8. L. Coderch, O. López, A. de la Maza, J. L. Parra, Am. J. Clin. Dermatol. 2003, 4, 107.
9. M. H. Meckfessel, S. Brandt, J. Am. Acad. Dermatol. 2014, 71, 177.
10. T. Hakozaki, L. Minwalla, J. Zhuang, M. Chhoa, A. Matsubara, K. Miyamoto, A. Greatens, G. G. Hillebrand, D. L. Bissett, R. E. Boissy, Br. J. Dermatol. 2002, 147, 20.
11. Q. S. Luu, Q. T. Nguyen, H. N. Manh, S. Yun, J. Kim, U. T. Do, K. Jeong, S. U. Lee, Y. Lee, Analyst. 2024, 149, 1068.
12. J.-P. Ortonne, D. L. Bissett, J. Investig. Dermatol. Symp. Proc. 2008, 13, 10.
13. J. B. Lee, M. Sung, M. Noh, J. E. Kim, J. Jang, S. J. Kim, J. W. Kim, Int. J. Pharm. 2020, 579, 119162.
14. J. Lee, M. Noh, J. Jang, J. B. Lee, Y.-H. Hwang, H. Lee, ACS Appl. Mater. Interfaces. 2022, 14, 36331.
15. R. R. Ong, C. F. Goh, Drug Deliv. Transl. Res. 2024, 14, 3512.
16. T. Haque, M. E. Lane, B. C. Sil, J. M. Crowther, D. J. Moore, Int. J. Pharm. 2017, 520, 158.
17. L. Wu, Y. Liu, X. Wang, M. Li, J. Li, X. Zhang, D. Gao, H. Li, Environ. Sci. Technol. 2024, 58, 8565.
18. P. Wei, K. Guo, W. Pu, Y. Xie, X. Huang, J. Zhang, Energy Fuels. 2020, 34, 1639.
19. Y. B. Monakhova, M. Betzgen, B. W. K. Diehl, Anal. Methods. 2016, 8, 7493.
20. A. Watts, in (Ed.: G. C. K. Roberts), Springer, Berlin Heidelberg, Berlin, Heidelberg 2013.
21. A. Mika, Z. Kaczynski, P. Stepnowski, M. Kaczor, M. Proczko-Stepaniak, L. Kaska, T. Sledzinski, Sci. Rep. 2017, 7, 15530.
22. T.-X. Meng, H. Ishikawa, K. Shimizu, S. Ohga, R. Kondo, J. Wood Sci. 2012, 58, 81.
23. R. J. Gillams, J. V. Busto, S. Busch, F. M. Goñi, C. D. Lorenz, S. E. McLain, J. Phys. Chem. B. 2015, 119, 128.
24. V. Bizot, E. Cestone, A. Michelotti, V. Nobile, in Cosmetics. 2017, 4.
25. J. A. Bouwstra, A. Nădăban, W. Bras, C. McCabe, A. Bunge, G. S. Gooris, Prog. Lipid Res. 2023, 92, 101252.
26. N. Monteiro, A. Martins, R. L. Reis, N. M. Neves, J. R. Soc. Interface. 2014, 11 (101), 20140459.
27. A. R. Mohammed, N. Weston, A. G. A. Coombes, M. Fitzgerald, Y. Perrie, Int. J. Pharm. 2004, 285 (1), 23.
28. T. Kondela, J. Gallová, T. Hauß, J. Barnoud, S.-J. Marrink, N. Kučerka Molecules 2017, 22 (12), 2078.